Talanta 85 (2011) 2159–2165

Contents lists available at ScienceDirect

Talanta

journal homepage: www.elsevier.com/locate/talanta

Screening analysis to detect adulteration in diesel/biodiesel blends using near infrared spectrometry and multivariate classification

Márcio José Coelho Pontes[a,*], Claudete Fernandes Pereira[b], Maria Fernanda Pimentel[c], Fernanda Vera Cruz Vasconcelos[a], Alinne Girlaine Brito Silva[b]

[a] Universidade Federal da Paraíba, Departamento de Química, João Pessoa, PB, Brazil
[b] Universidade Federal Rural de Pernambuco, Departamento de Química, Recife, PE, Brazil
[c] Universidade Federal de Pernambuco, Departamento de Engenharia Química, Recife, PE, Brazil

ARTICLE INFO

Article history:
Received 13 June 2011
Received in revised form 16 July 2011
Accepted 18 July 2011
Available online 23 July 2011

Keywords:
Diesel/biodiesel blends
Near infrared spectrometry
Screening analysis
Partial least squares-discriminant analysis
Linear discriminant analysis
Successive projections algorithm

ABSTRACT

This paper proposes an analytical method to detect adulteration of diesel/biodiesel blends based on near infrared (NIR) spectrometry and supervised pattern recognition methods. For this purpose, partial least squares discriminant analysis (PLS-DA) and linear discriminant analysis (LDA) coupled with the successive projections algorithm (SPA) have been employed to build screening models using three different optical paths and the following spectra ranges: 1.0 mm (8814–3799 cm^{-1}), 10 mm (11,329–5944 cm^{-1} and 5531–4490 cm^{-1}) and 20 mm (11,688–5952 cm^{-1} and 5381–4679 cm^{-1}). The method is validated in a case study involving the classification of 140 diesel/biodiesel blend samples, which were divided into four different classes, namely: diesel free of biodiesel and raw vegetal oil (D), blends containing diesel, biodiesel and raw oils (OBD), blends of diesel and raw oils (OD), and blends containing a fraction of 5% (v/v) of biodiesel in diesel (B5). LDA-SPA models were found to be the best method to classify the spectral data obtained with optical paths of 1.0 and 20 mm. Otherwise, PLS-DA shows the best results for classification of 10 mm cell data, which achieved a correct prediction rate of 100% in the test set.

1. Introduction

In 2005, the Brazilian government allowed the commercial use of biodiesel blends, introducing biodiesel in the Brazilian energy matrix. Initially, a volume fraction of 2% in conventional diesel (B2) was established, but in 2010 the biodiesel content in diesel fuel increased to 5% (B5), which is obligatory by law. According to the Brazilian National Agency for Petroleum Natural Gas, and Biofuels (ANP) regulations [1], the permitted maximum variation of biodiesel in B5 is ±0.5% (v/v).

Recently, the ANP has begun to develop means to avoid fuel adulteration. In the case of diesel/biodiesel blends, the main form of adulteration happens with the irregular addition of raw vegetable oils to diesel fuel. The use of these oils directly with engines can cause carbon deposits, injection blocking, and incomplete combustion, because of their high viscosities, low volatilities, and gum formation which is characteristic of oxidation and polymerization.

The European standard EN 14078 [2] for determining the biodiesel content in diesel fuel by using middle infrared (MIR) spectroscopy is an univariate method which measures the absorbance of the carbonyl stretching frequency at 1745 cm^{-1}. Vegetable oils also have carbonyl groups, however, that absorb in the same region (1745 cm^{-1}). The result obtained, therefore, by this method is compromised if the sample is adulterated with vegetable oils.

Considering the possibility of adulteration of biodiesel blends with vegetable oil, it is important to develop a method that is able to certify if the biodiesel blends are free of raw vegetable oil quickly, easily, and economically.

Recently, some methodologies have been developed to quantify vegetable oils in biodiesel blends using near infrared (NIR) and/or MIR spectrometry [3–5].

Pimentel et al. [3] developed multivariate calibration models based on MIR and NIR spectroscopy to determine the content of biodiesel in diesel fuel blends, considering the presence of raw vegetable oil. Additionally, the MIR region has also been used in a study involving principal component analysis (PCA) for rapid identification of diesel samples contaminated with raw vegetable oils.

Oliveira et al. [4] showed that the standard ASTM methods (ASTM 4052, ASTM D 445, ASTM D 4737, ASTM D 93, and ASTM

* Corresponding author at: Universidade Federal da Paraíba, Departamento de Química – Laboratório de Automação e Instrumentação em Química Analítica/Quimiometria (LAQA), CEP 58051-970, João Pessoa, PB, Brazil.
Tel.: +55 83 3216 7438; fax: +55 83 3216 7438.
E-mail addresses: marciocoelho@quimica.ufpb.br, marcio.quimica@gmail.com (M.J.C. Pontes).

0039-9140/$ – see front matter © 2011 Elsevier B.V. All rights reserved.
doi:10.1016/j.talanta.2011.07.064

D 86) recommended by the ANP to determine the quality of diesel/biodiesel blends are not suitable for detecting the adulteration of B2 or B5 blends with vegetable oils. The authors investigated the application of Fourier transform (FT) near infrared and FT-Raman spectrometry and multivariate calibration to determine adulterations of B2 and B5 blends with vegetable oils.

Soares et al. [5] used attenuated total reflection (ATR)-FTIR to quantify biodiesel adulteration with raw soybean oil. For this purpose, the authors developed multivariate PLS calibration models based on middle infrared (MIR) spectroscopy by using two classic variable selection methods: forward and stepwise. The results showed that this variable selection procedure improves not only the stability of the model with respect to the collinearity in multivariate spectra but also the interpretability of the relationship between the model and the sample composition.

In general, the works reported in the literature use only quantitative multivariate techniques such as principal component regression (PCR), or partial least square regression (PLS), or artificial neural network (ANN) to investigate biodiesel blends. Little research has been done to detect adulteration in these blends with vegetable oil using a procedure based on screening analysis [3,6].

The screening method of analysis is a process that identifies a compound or group of components in a sample with a minimum number of steps and the least manipulation of the sample. Conventional laboratory methods that provide detailed qualitative and quantitative information about samples are being increasingly (but not fully) replaced by rapid-response analytical tools providing a binary yes/no response, to indicate whether the target analytes are present above or below a pre-set concentration threshold. More basically, some important advantages can be achieved by using screening analysis: reduction of costs, rapidity, simplicity, and minimization of errors owing to delays between sampling and analysis [7,8].

Pattern recognition methods such as partial least squares discriminant analysis (PLS-DA) [9] and linear discriminant analysis (LDA) [10] have been applied extensively with screening analysis [11–14]. PLS-DA is based on the standard PLS algorithm and class labels are used as dependent y vector. In classification problems involving more than two classes, the PLS2 algorithm is generally used [9]. For instance, in data sets with four groups, each object is associated with one of the four following vectors [1,0,0,0], [0,1,0,0], [0,0,1,0] and [0,0,0,1], representing the classes 1, 2, 3 and 4, respectively. A value close to zero indicates that the new sample does not belong to the class under consideration and a value close to one indicates that it does. To determine the limit which an object is considered to be in a class or not, a threshold between zero and one is determined. When a value above the threshold is predicted, a sample is considered to belong to the class under study, while a value below the threshold indicates that the sample does not.

LDA, as proposed by Fisher [10], seeks a linear combination or function, D, of the independent variables to maximize the between-class variance relative to the within-class variance. The obtained latent variable is called a canonical variate. For k classes, $k-1$ canonical variates can be calculated. In order to have a well-posed problem, the number of training samples must be larger than the number of variables to be included in the LDA model. Therefore, the use of LDA to classify spectral data usually requires appropriate variable selection procedures [15–17]. The successive projections algorithm (SPA) [18–24] has been adopted for this purpose in the cases of a number of classification problems, including edible vegetable oils [20,25], diesel oils [20], Brazilian soils [26], cigarettes [27] and coffee [28] samples. The goal of SPA is to select variables with minimum multicollinearity and maximum information. The procedure for classification includes two phases. In the first, the variables are projected onto a subspace orthogonal to one variable as the reference, which is selected for each iteration. In the second phase, the best subset of variables is selected in order to minimize a cost function associated with the average risk G (Eq. (1)) of misclassification by LDA in a given validation set [19].

$$G = \frac{1}{Kv}\sum_{k=1}^{Kv} g_k \tag{1}$$

where g_k (risk of misclassification of the kth validation object $\mathbf{x}_k$) is defined as

$$g_k = \frac{r^2(\mathbf{x}_k, \boldsymbol{\mu}_{Ik})}{\min_{Ij \neq Ik} r^2(\mathbf{x}_k, \boldsymbol{\mu}_{Ij})} \tag{2}$$

In Eq. (2), the numerator $r^2(\mathbf{x}_k, \boldsymbol{\mu}_{Ik})$ is the squared Mahalanobis distance between object $\mathbf{x}_k$ (of class index Ik) and the sample mean $\boldsymbol{\mu}_{Ik}$ of its true class (both row vectors).

In the present paper, an analytical method to detect the adulteration of diesel/biodiesel blends with raw vegetable oils using NIR spectroscopy is proposed. For this, screening models based on supervised pattern recognition methods such as PLS-DA and LDA with variable selection by the SPA are employed. Three different optical paths and spectral ranges were evaluated: 1.0 mm (8814–3799 cm^{-1}), 10 mm (11,329–5944 cm^{-1} and 5531–4490 cm^{-1}) and 20 mm (11,688–5952 cm^{-1} and 5381–4679 cm^{-1}). The results obtained by two methods (PLS-DA and LDA/SPA) are assessed in terms of classification errors in a set of samples not used in the model-building process (test samples).

2. Experimental

2.1. Samples

One hundred and forty samples of four different classes were analyzed: diesel free of biodiesel and raw vegetal oil, D (35); blends containing diesel, biodiesel and raw oils, OBD (38); blends of diesel and raw oils, OD (35), and conforming samples which are composed by blends containing a fraction of 5% (v/v) of biodiesel, with variation of ±0.5% (v/v), B5 (32).

Blends were prepared using different oilseeds, animal fat and their respective esters. The biodiesel (B100) and oil samples were acquired in the market from different manufactures. B100 samples were analyzed and they are according to Brazilian specifications. In order to include variety in the diesel composition, the blends were taken from different samples of diesel fuel.

A mixture design with a central point for each kind of biodiesel, including internal points, was used to prepare the blends. Maximum and minimum levels of both biodiesel and oil were 0.0% and 10.0% (v/v). The ratio of ester/oil concentration was varied from 0.25 to 6.0.

2.2. NIR spectra measurements

The spectra were recorded by using a FTLA 2000–160 FTIR spectrophotometer (Bomem) and three different optical path lengths (1.0 mm, 10 mm and 20 mm). Each spectrum was obtained from an average of 32 scans in the range of 13,988–3799 cm^{-1} with a resolution of 8 cm^{-1}. The background spectra were obtained using a clean empty cell for each optical path. Temperature was controlled at 23 ± 1 °C throughout the spectral acquisition process.

2.3. Data analysis and software

The spectra were pre-treated using the Savitzky–Golay [29] first derivative procedure with a second-order polynomial (7-point window) and then divided into training, validation and test sets by

Table 1
Number of training, validation and test samples in each class.

Class	Sets		
	Training	Validation	Test
D	19	8	8
OBD	20	9	9
OD	19	8	8
B5	18	7	7
Total	76	32	32

using the classic Kennard–Stone (KS) algorithm [30]. The KS algorithm was applied to each class separately, as described in Ref. [20]. The number of samples in each set is presented in Table 1. All spectral data were mean-centered before modeling procedures.

The training and validation samples were used in the modeling procedures (including SPA variable selection for LDA and determination of factors number in PLS-DA models). In case of SPA, the validation samples were employed in order to select the best subset of wavenumbers by minimising a cost function defined as an average risk of misclassification by LDA, as described by Pontes et al. [20]. Therefore, the third set of test samples was used to check the generalization ability of the resulting classifier, as recommended elsewhere [31]. These samples can be deemed independent in that they were only used in the final evaluation and comparison of the classification models. The threshold value adopted for PLS-DA models was 0.5.

Spectrum differentiation, Savitzky–Golay smoothing, principal component analysis (PCA) and PLS-DA were carried out using Unscrambler® X.1 (CAMO S.A.). The KS and LDA-SPA algorithms were coded in Matlab® R2010a 7.10.0.499.

3. Results and discussion

3.1. NIR spectra

Fig. 1a–c presents the raw NIR spectra of the 140 samples in the range of 13,988–3799 cm^{-1} for each optical path studied. These NIR spectra show bands assigned to combinations (4800–4000 cm^{-1}, 7500–6700 cm^{-1}), first overtone (6300–5180 cm^{-1}), second overtone (8000–8910 cm^{-1}) and third overtone (11,270–10,360 cm^{-1}, Fig. 1c) regions of C–H stretching. In addition, the band assigned to second overtone of the C=O appears at about 5500 cm^{-1} and C–H stretch plus C=O stretch combination bands occur in the region of 4740–4370 cm^{-1} [32]. After a preliminary inspection of the spectra, those regions in which the signal of detector was saturated or poor signal-to-noise ratio were discarded, as indicated in Fig. 1a–c. The spectral ranges employed were: 8814–3799 cm^{-1} (1.0 mm), 11,329–5944 cm^{-1} and 5531–4490 cm^{-1} (10 mm), 11,688–5952 cm^{-1} and 5381–4679 cm^{-1} (20 mm).

3.2. Principal component analysis

Fig. 2 presents the PC2 × PC1 score plot resulting from the application of PCA to the derivative spectra using the three optical paths studied. As can be seen, there is a substantial dispersion and overlapping of the classes. More specifically this is true for the 10 mm optical path (Fig. 2b), where it is not possible to distinguish the blends (OD, OBD or B5) from conventional diesel samples (D).

3.3. LDA-SPA and PLS-DA classification

The optimum number of variables for the spectral data obtained using each optical path for LDA-SPA models was determined from the minimum of the cost function *G* [20] displayed in Fig. 3a–c. As can be seen, well-localized minimums are obtained for twelve, five and five variables when 1.0 mm, 10 mm and 20 mm optical paths were employed, respectively.

The variables selected by SPA for all optical lengths (1.0 mm, 10 mm and 20 mm) are presented in Fig. 4a–c. It can be observed that almost all wavenumbers selected are associated to both C–H stretching (4800–4000 cm^{-1}) and C–H plus C=O stretching (4740–4370 cm^{-1}) combination bands. The isolated wavenumber selected by SPA at 7491 cm^{-1} (Fig. 4a) may be associated to second combination region of CH stretching. The selected peaks at 5948 cm^{-1}, 5524 cm^{-1} (Fig. 4b) and 5987 cm^{-1}, 5956 cm^{-1} (Fig. 4c) are assigned to second overtone of the C=O and first overtone of CH stretching regions [32].

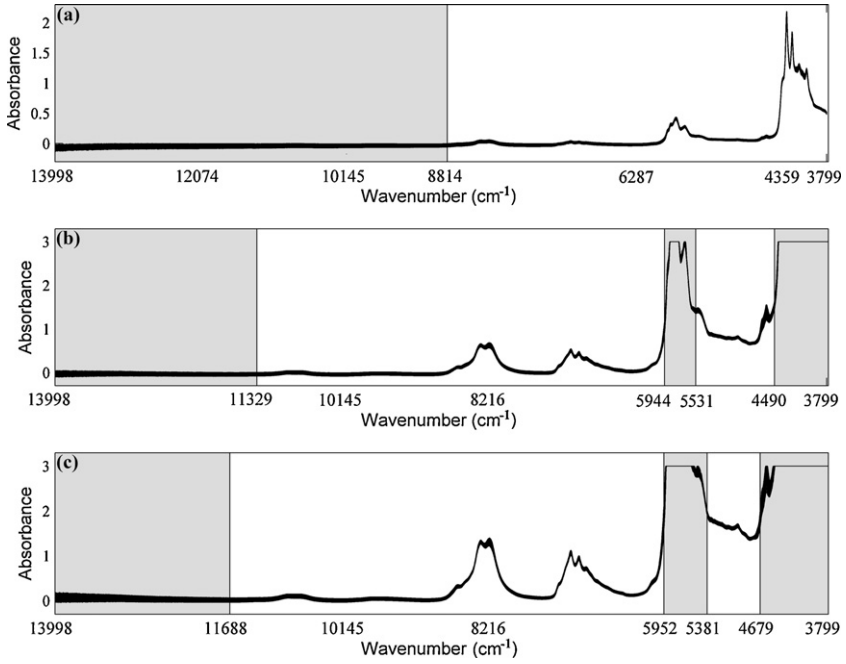

Fig. 1. Original NIR spectra of the 140 samples recorded in the (a) 1 mm, (b) 10 mm and (c) 20 mm optical paths. The regions highlighted in gray were discarded.

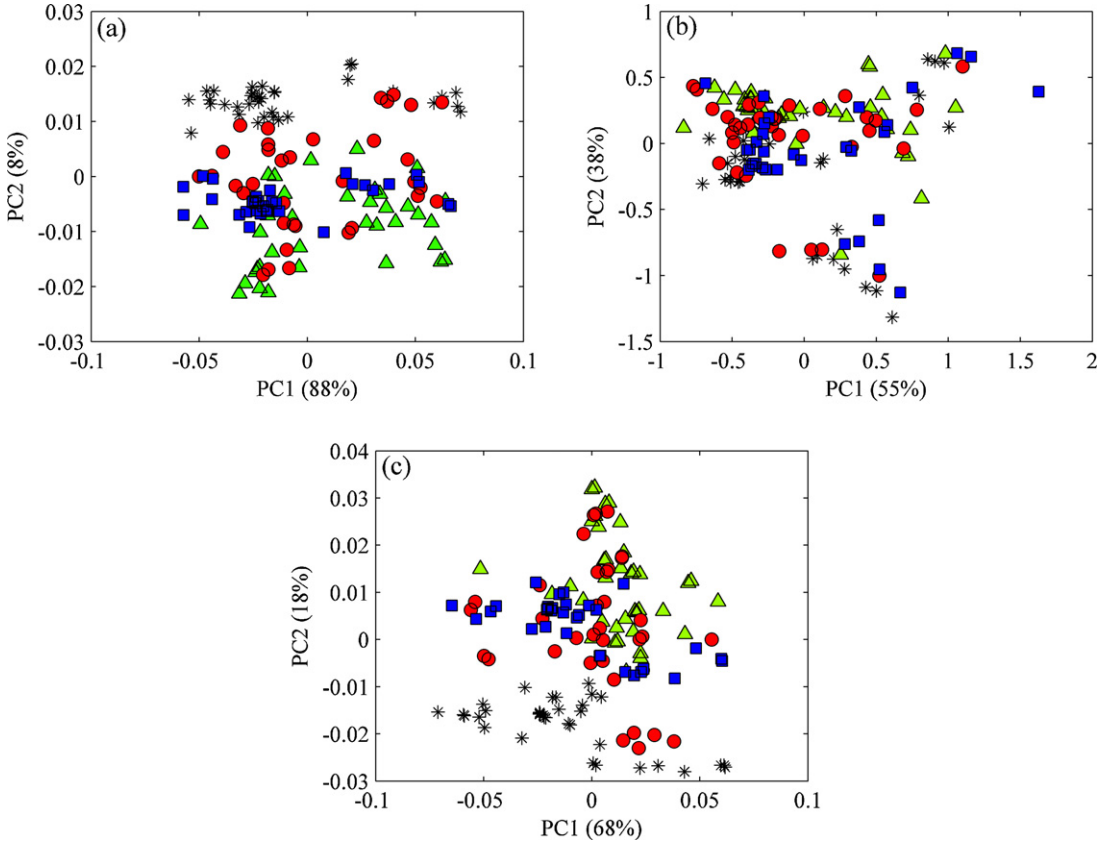

Fig. 2. PC2 × PC1 score plots for the overall data set (140 samples) in the optical path of (a) 1 mm, (b) 10 mm and (c) 20 mm (*: D; ▲: OBD; ●: OD and ■: B5). The percent variance explained by each PC is indicated in parenthesis.

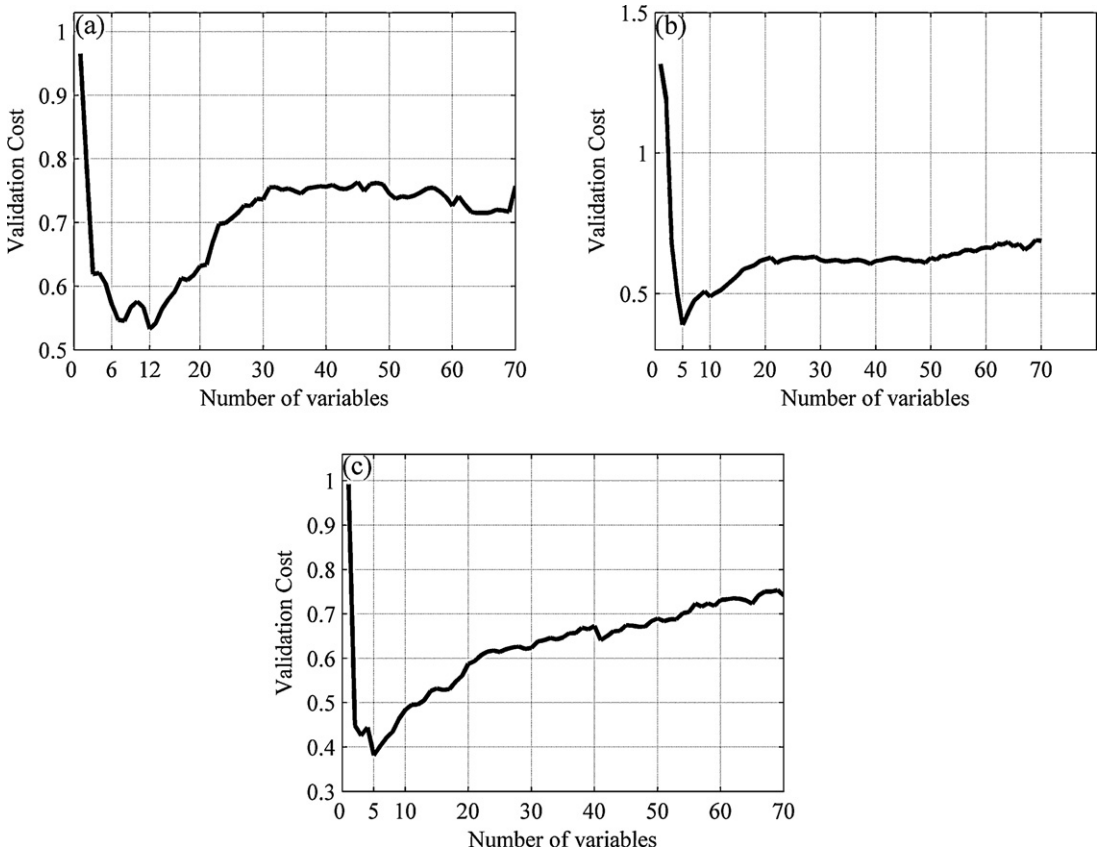

Fig. 3. Determination of the optimum number of variables in LDA-SPA for the optical path of (a) 1 mm, (b) 10 mm and (c) 20 mm.

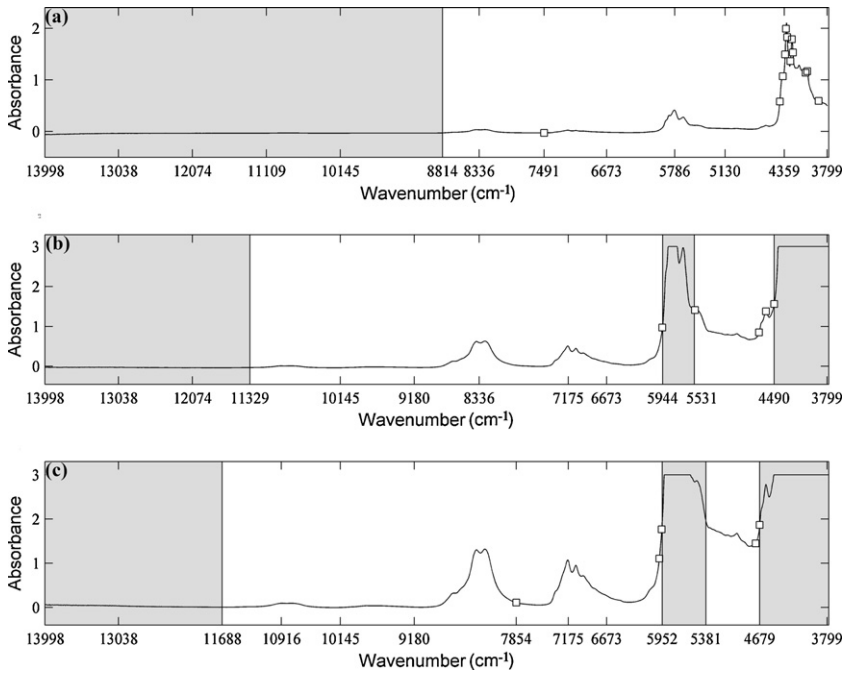

Fig. 4. Mean NIR spectra recorded in the optical path of (a) 1 mm, (b) 10 mm and (c) 20 mm with wavenumbers selected by SPA. The regions highlighted in gray were discarded before the modeling procedure.

The LDA models obtained with the variables selected by SPA were applied to the classification of the test set. Table 2 presents the classification errors of the LDA-SPA models applied to the test set using each optical path.

These results should be understood as follows: the two errors in the OBD row and 1.0 mm optical path OBD column, for instance, indicate that two OBD samples were incorrectly classified by the LDA-SPA model using the optical path of 1.0 mm. One of these

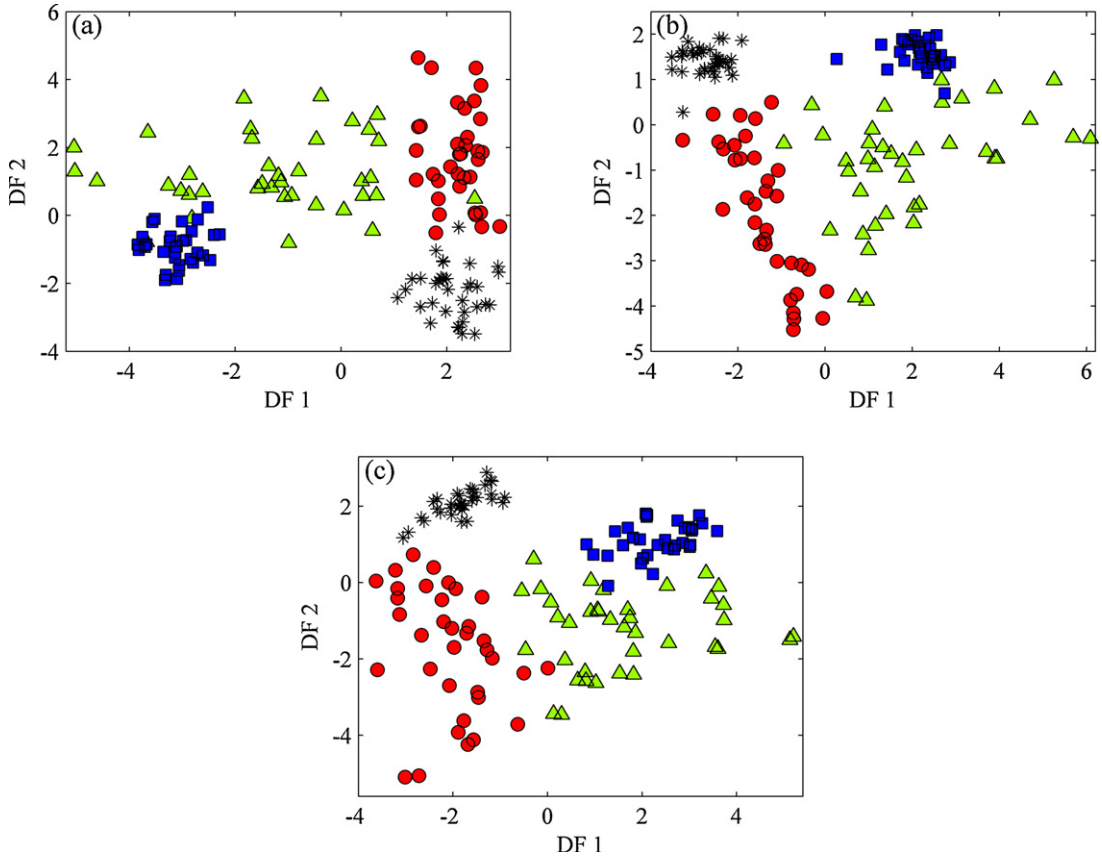

Fig. 5. DF2 × DF1 score plots for the overall data set (140 samples) using optical path of (a) 1 mm, (b) 10 mm and (c) 20 mm (*: D; ▲: OBD; ●: OD and ■: B5).

Table 2
Number of classification errors of the LDA-SPA models in the test set for 1 mm, 10 mm and 20 mm optical lengths. The number of selected wavenumber by SPA is indicated in parenthesis. *N* is the number of test samples in each class.

True class	*N*	⌀ = 1 mm LDA-SPA model (12)				⌀ = 10 mm LDA-SPA model (5)				⌀ = 20 mm LDA-SPA model (5)			
		D	OBD	OD	B5	D	OBD	OD	B5	D	OBD	OD	B5
D	8	–	–	–	–	–	–	–	–	–	–	–	–
OBD	9	–	2	1	1	–	2	–	2	–	1	1	–
OD	8	1	–	1	–	–	–	–	–	–	–	–	–
B5	7	–	–	–	–	–	–	–	–	–	–	–	–

Table 3
Number of classification errors of the PLS-DA models in the test set for 1 mm, 10 mm and 20 mm optical lengths. The number of latent variable in each PLS-DA model is indicated in parenthesis. *N* is the number of test samples in each class.

True class	*N*	⌀ = 1 mm PLS-DA model (7)				⌀ = 10 mm PLS-DA model (16)				⌀ = 20 mm PLS-DA model (8)			
		D	OBD	OD	B5	D	OBD	OD	B5	D	OBD	OD	B5
D	8	–	–	–	–	–	–	–	–	–	–	–	–
OBD	9	–	3	1	2	–	–	–	–	–	2	2	–
OD	8	1	–	1	–	–	–	–	–	–	–	–	–
B5	7	–	–	–	–	–	–	–	–	–	–	–	–

samples was classified as belonging to the OD class and one was classified as belonging to the B5 class.

The best result for the LDA/SPA models was obtained with the 20 mm optical path, which correctly classified 31 of the 32 test samples. This outcome corresponds to a correct prediction rate of 97%. All conforming samples, which are composed of blends containing a fraction of 5% (v/v) of biodiesel (B5 authentic), were correctly classified in their own class. The sample that was misclassified (OBD classified as OD) is a blend containing a fraction of 8% (v/v) of used sunflower oil and a fraction of 2% (v/v) of its corresponding biodiesel.

The satisfactory classification performance of LDA-SPA is further demonstrated by Fig. 5a–c, which presents the scores of the first two discriminant functions (DF2 × DF1) for the overall data set using the three optical paths (1.0 mm, 10 mm and 20 mm). It is possible to observe that B5 authentic and pure diesel (D) samples are separated from samples contaminated with vegetable oil (OD and OBD) along the DF2 direction. DF1 clearly distinguishes B5 samples from D and OD class (Fig. 5a–c).

PLS-DA models were also built for the four classes (D, OBD, OD and B5) using the spectral data obtained with optical paths of the 1.0 mm, 10 mm and 20 mm. The resulting classification errors obtained in the test set are presented in Table 3.

The PLS-DA method classified satisfactorily the samples for all optical paths studied. In particular, the best result was obtained using the 10 mm optical path, which correctly classified all samples in the test set.

Tables 2 and 3 reveal that the use of LDA-SPA models provided a better classification of the spectral data obtained using 1.0 mm and 20 mm optical paths, when compared with the PLS-DA. For the 10 mm optical path, however, the best results were obtained from PLS-DA which achieved a correct prediction rate of 100% in the test set.

4. Conclusions

This paper presented a method based on screening analysis for detection of adulteration in diesel/biodiesel blends employing NIR spectrometry and multivariate classification such as PLS-DA and LDA-SPA.

A PCA study applied to the different optical paths (1.0 mm, 10 mm and 20 mm) revealed a substantial overlapping among all classes. In contrast, LDA with wavenumbers selected by SPA was able to identify raw oil contamination and illegal blends of diesel containing raw oil instead of biodiesel.

The LDA-SPA models provided a better classification performance using the data obtained from the 1.0 mm and 20 mm optical paths, when compared with the PLS-DA. More specifically, the data set recorded using a 20 mm optical path achieved a correct prediction rate of 97%. Using the 10 mm optical path, however, the best results were obtained from PLS-DA which correctly classified all samples in the test set.

The results obtained in this investigation suggest that the proposed method is a promising alternative to detect adulteration in diesel/biodiesel blends. It is worth noting that the method is based solely on spectroscopic measurements and chemometric techniques. Moreover, after the screening models have been obtained, the proposed methodology can be applied to new samples in a fast and straightforward manner.

Acknowledgments

This work was supported by FACEPE, FINEP, CNPq, CAPES and INCTAA. The authors are also grateful to TRANSPETRO S.A. (Suape/PE) for providing the pure diesel samples employed in this study.

References

[1] Brazilian National Agency for Petroleum Natural Gas, and Biofuels (ANP). Resolution no. 42, DE 16.12.2009. Available from: http://www.anp.gov.br (accessed on 20.12.10.).
[2] European Standard – EN 14078:2009, Liquid Petroleum Products – Determination of Fatty Methyl Ester (FAME) Content in Middle Distillates – Infrared Spectrometry Method.
[3] M.F. Pimentel, G.M.G.S. Ribeiro, R.S. Cruz, L. Stragevitch, J.G.A. Pacheco Filho, L.S.G. Teixeira, Microchem. J. 82 (2006) 201.
[4] F.C.C. Oliveira, C.R.R. Brandão, H.F. Ramalho, L.A.F. Costa, P.A.Z. Suarez, J.C. Rubim, Anal. Chim. Acta 587 (2007) 194.
[5] I.P. Soares, T.F. Rezende, R.C. Silva, E.V.R. Castro, I.C.P. Fortes, Energy Fuels 22 (2008) 2079.
[6] C.N.C. Corgozinho, V.M.D. Pasa, P.J.S. Barbeira, Talanta 76 (2008) 479.
[7] R. Munõz-Olivas, Trends Anal. Chem. 23 (2004) 203.
[8] R.S. Costa, S.R.B. Santos, L.F. Almeida, E.C.L. Nascimento, M.J.C. Pontes, R.A.C. Lima, S.S. Simões, M.C.U. Araújo, Microchem. J. 78 (2004) 27.
[9] R.G. Brereton, Chemometrics for Pattern Recognition, John Wiley & Sons Ltd., Bristol, UK, 2009.
[10] R.A. Fisher, Ann. Eugenics 7 (1936) 179.
[11] M.-T. Sánchez, D.P. Marín, K.F. Rojas, J.-E. Guerrero, A.G. Varo, Talanta 78 (2009) 530.

[12] O. Galtier, O. Abbas, Y.L. Dréau, C. Rebufa, J. Kister, J. Artaud, N. Dupuy, Vib. Spectrosc. 55 (2011) 132.
[13] M.C. Ortiz, L. Sarabia, R. García-Rey, M.D.L. Castro, Anal. Chim. Acta 558 (2006) 125.
[14] P. Williams, P. Geladi, G. Fox, M. Manley, Anal. Chim. Acta 653 (2009) 121.
[15] Y. Mallet, D. Coomans, O. de Vel, Chemom. Intell. Lab. Syst. 35 (1996) 157.
[16] A.R. Caneca, M.F. Pimentel, R.K.H. Galvão, C.E. Matta, F.R. Carvalho, I.M. Raimundo Jr., C. Pasquini, J.J.R. Rohwedder, Talanta 70 (2006) 344.
[17] M. Casale, N. Sinelli, P. Oliveri, V.D. Egidio, S. Lanteri, Talanta 80 (2010) 1832.
[18] M.C.U. Araújo, T.C.B. Saldanha, R.K.H. Galvão, T. Yoneyama, H.C. Chame, V. Visani, Chemom. Intell. Lab. Syst. 57 (2001) 65.
[19] R.K.H. Galvão, M.C.U. Araújo, in: S.D. Brown, R. Tauler, B. Walczak (Eds.), Comprehensive Chemometrics: Chemical and Biochemical Data Analysis, Elsevier, Oxford, 2009, p. 233.
[20] M.J.C. Pontes, R.K.H. Galvão, M.C.U. Araújo, P.N.T. Moreira, O.D. Pessoa Neto, G.E. José, T.C.B. Saldanha, Chemom. Intell. Lab. Syst. 78 (2005) 11.
[21] M.S. Di Nezio, M.F. Pistonesi, W.D. Fragoso, M.J.C. Pontes, H.C. Goicoechea, M.C.U. Araujo, B.S. Fernández Band, Microchem. J. 85 (2007) 194.
[22] M.F. Pistonesi, M.S. Di Nezio, M.E. Centurión, A.G. Lista, W.D. Fragoso, M.J.C. Pontes, M.C.U. Araujo, B.S. Fernández Band, Talanta 83 (2010) 320.
[23] A.F.C. Pereira, M.J.C. Pontes, F.F.G. Neto, S.R.B. Santos, R.K.H. Galvão, M.C.U. Araújo, Food Res. Int. 41 (2008) 341.
[24] M.J.C. Pontes, A.M.J. Rocha, M.F. Pimentel, C.F. Pereira, Microchem. J. 98 (2011) 254.
[25] F.F. Gambarra-Neto, G. Marino, M.C.U. Araújo, R.K.H. Galvão, M.J.C. Pontes, E.P. Medeiros, R.S. Lima, Talanta 77 (2009) 1660.
[26] M.J.C. Pontes, J. Cortez, R.K.H. Galvão, C. Pasquini, M.C.U. Araújo, R.M. Coelho, M.K. Chiba, M.F. Abreu, B.E. Madari, Anal. Chim. Acta 642 (2009) 12.
[27] E.D. Moreira, M.J.C. Pontes, R.K.H. Galvão, M.C.U. Araújo, Talanta 79 (2009) 1260.
[28] U.T.C.P. Souto, M.J.C. Pontes, E.C. Silva, R.K.H. Galvão, M.C.U. Araújo, F.A.C. Sanches, F.A.S. Cunha, M.S.R. Oliveira, Food Chem. 119 (2010) 368.
[29] A. Savitzky, M.J.E. Golay, Anal. Chem. 36 (1964) 1627.
[30] R.W. Kennard, L.A. Stone, Technometrics 11 (1969) 137.
[31] F. Marini, F. Balestrieri, R. Bucci, A.D. Magri, A.L. Magri, D. Marini, Chemom. Intell. Lab. Syst. 73 (2004) 85.
[32] J. Workman, L. Weyer, Pratical Guide to Interpretative Near-Infrared Spectroscopy, CRC Press, New York, 2008.